Non-Tidal Ocean Loading Signals of the North and Baltic Sea From Terrestrial Gravimetry, GNSS, and High-Resolution Modeling

C. Voigt[1] , R. Sulzbach[1,2] , H. Dobslaw[1] , A. Weise[3], L. Timmen[3], Z. Deng[1], M. Reich[1] , N. Stolarczuk[1], H. Peters[4], M. Fietz[4], M. Thomas[1,2], and F. Flechtner[1,5]

[1]Helmholtz Centre Potsdam—GFZ German Research Centre for Geosciences, Potsdam, Germany, [2]Institute of Meteorology, Freie Universität Berlin (FUB), Berlin, Germany, [3]Institute of Geodesy, Leibniz Universität Hannover (LUH), Hannover, Germany, [4]Biologische Anstalt Helgoland, Alfred-Wegener-Institute (AWI), Helmholtz Centre for Polar and Marine Research, Helgoland, Germany, [5]Institute of Geodesy and Geoinformation Science, Technische Universität Berlin (TUB), Berlin, Germany

Abstract Non-tidal ocean loading (NTOL) signals are known to be a significant source of geophysically induced noise in gravimetric and geodetic observations also far-away from the coast and especially during extreme events such as storm surges. Operationally available corrections suffer from a low temporal and spatial resolution and reveal too small amplitudes on continental stations. Dedicated high-resolution sea-level modeling of the North and Baltic Sea provides an improved prediction of NTOL signals. Superconducting gravimeter and Global Navigation Satellite Systems observations on the small offshore island of Heligoland in the North Sea are used for an evaluation of the model values revealing largely increased correlations of up to 0.9 and signal reductions of up to 50% during a storm surge period of one month in January and February 2022. Evaluations on additional continental superconducting gravimeter stations also show significant improvements through the recommended high-resolution modeling for improved signal separation further away from the coast.

Plain Language Summary Terrestrial gravimetry is a technique to monitor temporal variations of the gravity acceleration at the Earth's surface that are induced by mass variations and deformations caused by a large number of geophysical effects on very different temporal and spatial scales. Current applications of high social relevance are the estimation of terrestrial water storage variations under climate change conditions, for example, groundwater depletion or polar and alpine ice mass loss, as well as hazard and geothermal monitoring. Before analyzing such signals of interest, it is essential to separate all other signals included in the gravimetric observations usually on the basis of adequate models. Amongst these disturbing signals, NTOL is one of the smaller but still significant effects. Up to now, the available operational corrections show a weak correlation with gravimetric observations and their application does not lead to a significant reduction of the observational signal variation. This situation largely improves with a high-resolution model for gravity observations on the North Sea island of Heligoland. The model results are also applied to gravity records that were observed further away from the coast to assess the benefits of the model for an improved signal separation even at continental stations.

1. Introduction

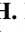Gravimetric observations at the Earth's surface are affected by mass variations and deformations of the Earth's crust induced by a large number of geophysical effects. While solid Earth tides and ocean tide loading (OTL) are usually estimated from local tidal analyses of the gravimetric observations, the effects of atmospheric mass-redistributions and Earth rotation are computed by various services. Non-tidal ocean loading (NTOL) signals, largely caused by wind-driven surges, are distinct at the coast, but through their large-scale characteristics significantly affect gravimetric and geodetic observations up to several 100 km away from the coast. Hence, for the analysis of terrestrial water storage variations or hazard and geothermal monitoring on local or regional scales, the NTOL signals should be reduced from the observations, provided that the quality of the NTOL signals is sufficient. At present, two operational products based on global ocean models are available for terrestrial gravimetry that are both limited in temporal and spatial resolution: The EOST loading service (Boy, 2024) provides daily NTOL model predictions based on the global ocean model ECCO2 in 0.25° resolution, while the MATLAB toolbox mGlobe (Mikolaj et al., 2016) allows for the computation of NTOL predictions from ocean

Validation: C. Voigt, A. Weise,
L. Timmen
Visualization: C. Voigt
Writing – original draft: C. Voigt
Writing – review & editing: C. Voigt,
R. Sulzbach, H. Dobslaw, A. Weise,
L. Timmen, Z. Deng, M. Reich,
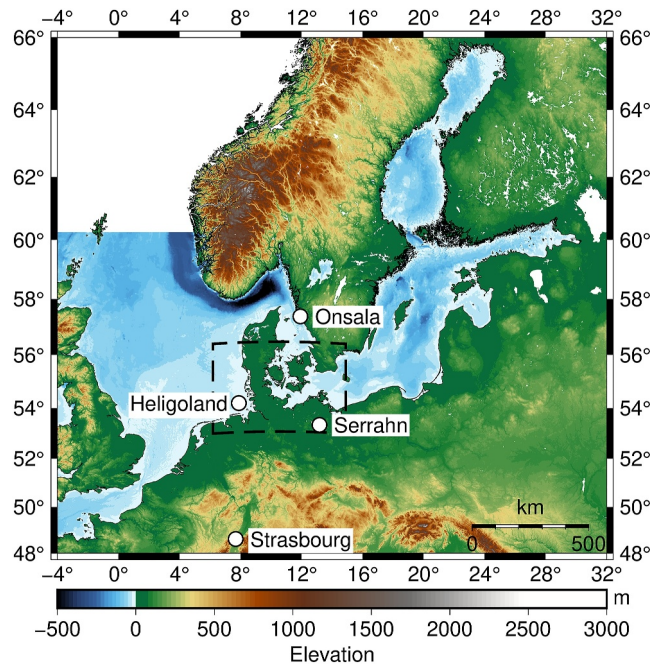N. Stolarczuk, H. Peters, M. Thomas,
F. Flechtner

Figure 1. The bathymetry of the North and Baltic Sea areas covered by the ocean model BSH-HBMnoku and adjacent topography with the four superconducting gravimeter stations under investigation. The dashed box indicates the fine resolution area of the model.

bottom pressure anomalies of the GRACE Atmosphere and Ocean De-Aliasing Level-1B (AOD1B RL07 and predecessor products) in 3 hr sampling up to spherical harmonic degree and order (d/o) 180 (Dobslaw et al., 2017; Shihora et al., 2022). In general, both operational products show a weak correlation with gravimetric observations and their application does not lead to a significant reduction of the observational signal variation.

The separation of NTOL signals from gravimetric observations has two limitations: First, superconducting gravimeters are usually installed far away from the coasts in order to keep the disturbing signals from the oceans small. Second, NTOL signals are often superimposed by significant terrestrial water storage variations, since wind surges are often accompanied by heavy precipitation events. To tackle these challenges, the small offshore island of Heligoland in the North Sea (Figure 1) was chosen as study site (Voigt et al., 2023; Weise et al., 2020). It is equipped with a redundant set of continuously operating sensors: two gravimeters, two Global Navigation Satellite Systems (GNSS) stations as well as two tide gauge stations.

Maximum NTOL signals of the North Sea were predicted by Fratepietro et al. (2006) with gravity increases of 80 nm/s^2 and vertical displacements of 30 mm downwards during a storm surge on 30 January 2000 with a local sea level of 2.7 m above mean high water (MHW) based on the Proudman Oceanographic laboratory storm surge model (POLSSM) with a resolution of approx. 12 km. The authors found some evidence of storm surge loading in the superconducting gravimeter (SG) data of Membach, which is 200 km away from the coast, and recommended a SG installation closer to the coast for NTOL signal enhancement. An extension of this study is provided by Boy and Lyard (2008), who applied 3D atmospheric modeling from the European Center for Medium-range Weather Forecasts (ECMWF) and sea surface heights from the Toulouse Hydrodynamic Unstructured Grid Ocean model (HUGO-m). They analyzed the NTOL signals on 8 SG stations in Central Europe during two storm surge periods of 2 weeks, again January and February 2000 and in addition December 2003, with largely improved correlations of up to 0.8 between gravity and NTOL model predictions. Fenoglio-Marc et al. (2015) find vertical displacements of 3–5 cm during a storm surge in December 2013 from a GNSS network of the German North Sea coast and provide maximum correlations of 0.95 between GNSS and ocean models at Heligoland with signal reductions of up to 61% for a period of 2 days when correcting the observations with the model values.

The primary objective of this study is to provide an improved quantification of NTOL signals of the North and Baltic Sea with a special focus on storm surges in the German Bight. The improvement of the state of the art is
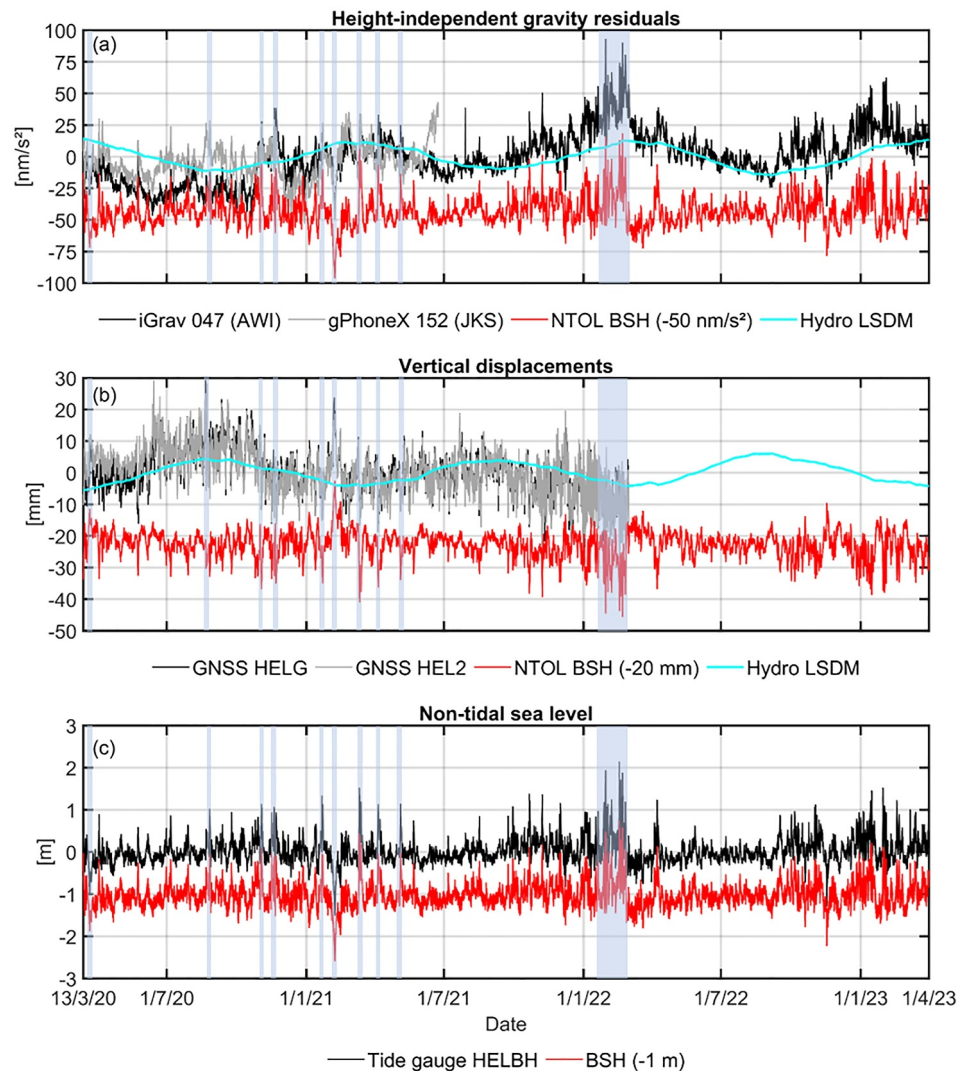
Figure 2. Available data on the island of Heligoland: (a) height-independent gravity residuals from iGrav 047 (AWI) and gPhoneX 152 (JKS), (b) vertical displacements (positive upwards) from Global Navigation Satellite Systems stations HEL2 and HELG, corresponding values from BSH ocean model and LSDM hydrological model both evaluated at $H_0 = 0$ m, and (c) the non-tidal sea level from local tide gauge HELBH and BSH model. Marked in light blue are the periods under investigation, that is, nine single weeks in the common gravimeter period with wind surges between 1.0 and 1.5 m deviation from mean high or low water, and an extreme month with several storm surges of more than 1.5 m above mean high water in January and February 2022. Please note that the BSH model values are shifted vertically to ease readability.

achieved through two key points. First, we predict the NTOL signals from the regional high-resolution operational ocean model BSH-HBMnoku (Brüning et al., 2021). Second, for the evaluation of the NTOL model predictions, we set up a SG and use specially processed GNSS data on the island of Heligoland to provide maximum NTOL signals. In this way, we achieve largely increased correlations and signal reductions between regional model predictions and observations that are compared with the results from presently available global operational products AOD7 and ECCO2, and also at additional continental SG stations at Onsala, Serrahn and Strasbourg.

2. Data and Methodology

The de-tided and reduced data sets of gravimeters, GNSS sensors and tide gauges at Heligoland are shown in Figure 2 in terms of gravity residuals, vertical displacements and non-tidal sea level variations, respectively, for their available time periods. Details on the data sets, the study site and the methodology can be found in Voigt et al. (2023), while all data reduction steps are described in the following.

The continuously operating gravimeters iGrav 047 at Alfred-Wegener-Institute (AWI) at $H_0 = 2.31$ m above mean sea level and the gPhoneX 152 at James-Krüss-Schule (JKS) at $H_0 = 41.35$ m are used for cross-validation over a period of 15 months. Due to rather small distances to the coast of 15 and 230 m, respectively, the observations of both gravimeters at different heights are strongly affected by the direct Newtonian attraction of local water mass variations in the North Sea (see also Olsson et al., 2009). The empirical reduction of this local Newtonian attraction from the gravimetric observations is done on the basis of the local tide gauge measurements resulting in height-independent gravity observations ($H_0 = 0$ m). It should be noted that the transfer function between the local sea level and the height-dependent gravity component for iGrav 047 (AWI) from Voigt et al. (2023) has been slightly modified for this study analyzing storm surges and sea level heights exceeding the gravimeter height. After reduction of the height-dependent gravity component, the two gravimetric time series are expected to provide identical signals within their uncertainty budgets.

These height-independent gravity observations with 1 hr time sampling are further reduced by the effects of solid Earth tides and OTL on the basis of local tidal analyses (3 years of iGrav and 16 months of gPhoneX data) with the ET34-X-V80 software (Schueller, 2015, 2020), atmospheric mass-redistributions from the Atmospheric Attraction Computation Service (ATMACS; Klügel & Wziontek, 2009) but without the very recently added NTOL term, which accounts for the attraction of the inverted barometer response to the ocean (Antokoletz et al., 2024), and Earth rotation based on the Earth Orientation Parameters (EOPs) provided by the International Earth Rotation and Reference Systems Service (IERS). The vertical displacements in 1 hr time sampling from the GNSS stations HELG and HEL2 are processed using the Precise-Point-Positioning (PPP) method and random-walk constrain described in Deng (2023), while the reductions are done according to the IERS conventions 2010. This solution is specifically designed for the analysis of NTOL signals with short duration, and thus contains occasional artificial jumps of up to 10 mm in the coordinate time series at day boundaries. The sea level heights of tide gauge HELBH in the inland harbor next to iGrav 047 (AWI) are de-tided by a local tidal analysis based on 22 years of observations with ET34-X-V80 while the tide gauge HELSH located at the south harbor of Heligoland has been found to be affected by instrumental issues and natural disturbances (swell, seiches, wind waves), and thus discarded from further study.

Both gravity residuals and GNSS vertical displacements in Figures 2a and 2b are dominated by short-term fluctuations that can be attributed primarily to wind surges according to Figure 2c. On seasonal time scale, the gravity residuals from iGrav 047 (AWI) and the GNSS vertical displacements show variations attributed to continental water storage variations from the mainland, while these do not show up significantly in the gPhoneX 152 time series due to the irregular drift. This is supported by the crustal deformations from the Land Surface Discharge Model (LSDM; Dill, 2008) calculated as described in Dill and Dobslaw (2013) and depicted in Figure 2. No significant gravity response could be detected during and after precipitation events due to the limited natural storage capacity of the island's soil. Hence, most of the precipitation in the vicinity of the gravimeter sites occurs as surface runoff and flows immediately or after a very short delay into the sea. On time scales of a few days, the main target of this study, NTOL signals should be the primary source of gravity variations, especially during storm surges.

The shallow-water equation model BSH-HBMnoku covers the North Sea up to a longitude of 4° West and up to a latitude of 60°15' North and the full Baltic Sea (Figure 1). The horizontal resolution is 3 sea miles (5 km), which is densified along the German coasts to 0.5 sea miles (0.9 km). The model is available since 1 January 2016 to 5 days in advance with a temporal resolution of 15 min. The computation of the NTOL model predictions is done as follows. We use hourly snapshots of the sea surface height anomalies from the BSH model and 3-hourly snapshots of AOD7 (1/2° resolution) for the domain indicated in Figure 1 and perform first-order conservative remapping with the Climate Data Operator (CDO) software (Schulzweida, 2022) to a resolution of 1/8°. The obtained load grids and the Gutenberg–Bullen Earth model are used as input for the function NLOADF of the software package SPOTL (Agnew, 2013). The convolution of the Green's functions with the load grids is performed for all timesteps and for each gravimeter station, while the height of station Heligoland is set to zero to obtain the height-independent gravity signatures (Voigt et al., 2023). As the BSH model contains both tidal and non-tidal sea level variations, the BSH model predictions are de-tided on the basis of 3 years of data with ET34-X-V80 using the same tidal wave grouping as for the observations.

In addition to Heligoland, three additional SG stations are chosen to evaluate the NTOL models according to the following two criteria: short distances to the North and Baltic Sea coasts and data availability of gravity residuals

for 1 month with several storm surges from 26 January to 25 February 2022. From the database of the International Geodynamics and Earth Tide Service (IGETS; Voigt et al., 2016), the SG stations at Onsala, Serrahn and Strasbourg are selected. The processing and description of gravity residuals (Level 3 data) is described in Boy et al. (2020).

3. Results

In order to highlight different features of the gravimetric monitoring on Heligoland, we focus on three different analysis periods corresponding to a step-wise amplification of the NTOL signals and provide correlations and signal reductions between model predictions and observations. During all comparisons, any offsets between the data sets are reduced for the computation of RMS differences.

3.1. Common Observation Period at Heligoland

First, we cross-validate the redundant set of gravimeters and GNSS sensors. The comparison of height-independent gravity residuals from iGrav 047 (AWI) and gPhoneX 152 (JKS) reveals a RMS difference of 15 nm/s^2 over the full common period of 15 months from 13 March 2020 to 23 June 2021. These differences include measurement uncertainties from both gravimeters and the tide gauge used for the reduction of the individual height-dependent gravity components, as well as specific local hydrological signals around the gravimeter sites, while atmospheric and large-scale hydrological signals are identical for both instruments and thus cancel out in the differences. The primary source for remaining differences is, however, the highly irregular drift of the gPhoneX, underlining that such spring gravimeters should rather not be used for the monitoring of geophysical signals with periods of some months.

The comparison of the vertical displacements from the GNSS stations HEL2 and HELG provides a RMS difference of 3 mm over the full common period. In contrast to the gravimetric data sets, the uncertainties of the vertical displacements from the two GNSS solutions are highly correlated due to common systematic effects induced by, for example, observing the same satellites at the same times. In total, the uncertainty of the 1 hr vertical displacements from the GNSS solutions appears to be at the level of 1 cm. The correlations between the height-independent gravity residuals and the vertical displacements are up to −0.66 for iGrav 047 (AWI) and -0.30 for gPhoneX 152 (JKS), respectively. This again corroborates deficiencies of the gPhoneX on longer time scales, but also reflects strong common signals in both iGrav and GNSS time series, namely the large-scale NTOL.

The comparison of the observational gravity residuals with the predicted signals from the BSH model over the full common period reveals correlations of 0.50 and 0.45 as well as signal reductions of 8% and 6% when subtracting the NTOL predictions of the BSH model from the gravity residuals of iGrav 047 (AWI) and gPhoneX 152 (JKS), respectively. For GNSS, the results are slightly better with correlations of 0.55 between GNSS vertical displacements and BSH model as well as signal reductions of 15%. The smaller reduction of the gravity residuals is caused by residual local uncertainties still included in the time series, while GNSS is not sensitive to local effects but only to the elastic deformation of the crust, which effectively acts as a spatial low-pass filter where even highly localized time-variable surface loads (like artificial water reservoirs) cause spatially correlated deformations many kilometers away.

3.2. Nine Single Weeks Within the Common Observation Period With Strong Wind Surge Events at Heligoland

Secondly, we show some examples of exceptionally strong NTOL signals by focusing on nine single weeks with wind surge leading to sea-level anomalies of up to 1.5 m (Figure 2c). The RMS difference of iGrav and gPhone improves drastically by a factor of 5 to 3 nm/s^2 in average for the nine periods compared to the full common period, showing that the irregular drift of the gPhone is the limiting factor on long time scales. The RMS difference of the GNSS vertical displacements, however, has only decreased slightly to 2 mm compared to the full common period. The signal-to-noise ratio is better for gravimetry than GNSS for these 1-week intervals suggesting that the wind surge signals over some hours can be resolved more precisely by gravimetry. The correlations between the gravity residuals and GNSS vertical displacements is now −0.70 for all sensor combinations.
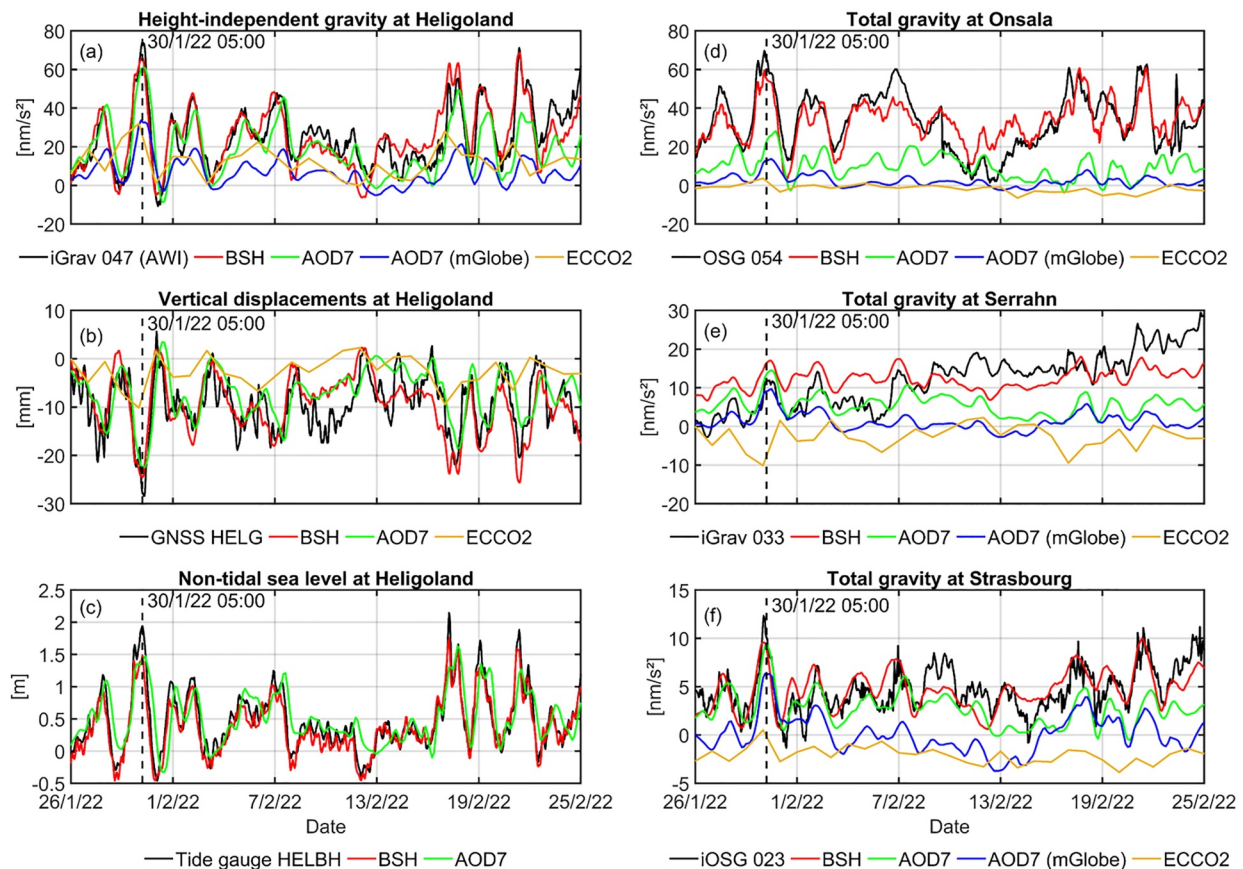
Figure 3. Gravity, Global Navigation Satellite Systems and tide gauge observations at Heligoland with corresponding non-tidal ocean loading (NTOL) model values during 1 month with several storm surges (a–c), gravity residuals from SG stations at Onsala, Serrahn and Strasbourg with corresponding NTOL model values (d–f). The observations are fitted to the mean values of the corresponding values from the BSH model.

Correlations between gravity residuals and the BSH model are 0.82 and 0.85 for these nine single weeks, while the signal reduction of the gravity residuals by subtracting the NTOL predictions of the BSH model are 32% and 39% for iGrav and gPhone, respectively. These figures show that the gPhone can be used adequately for such time intervals. GNSS vertical displacements are correlated with BSH model values by 0.73 (HEL2) and 0.75 (HELG) and signals can be reduced by 33% on both GNSS stations. In total, these comparisons during single weeks with intense winds further support the conclusion that the observed gravity signals are primarily driven by NTOL.

3.3. One Month With Several Storm Surges in the German Bight

In a third step, we extend the analysis to 1 month with several storm surges in the German Bight from 26 January to 25 February 2022, and do not only focus on Heligoland but also on three additional SG stations on the continent. Between 30 January and 7 February 2022, six storm surges with at least +1.5 m hit the North Sea coast of Germany. Shortly afterward from 17 to 22 February 2022, seven additional storm surges induced strong sea-level variations (Figure 3c). At 30 January 2022 at 05:00 UTC, maximum storm surge signals reach gravity increases (peak-to-peak) of up to 85 nm/s^2 and vertical displacements of -34 mm from superconducting gravimeter iGrav 047 (AWI) and GNSS HELG observations at Heligoland, respectively, during increased local sea level heights of +2.0 m above mean high water at Heligoland. These figures are even larger than the maximum values reported previously by Fratepietro et al. (2006).

The correlations at Heligoland are 0.87 and 0.74 for gravimetry and GNSS, respectively, with the BSH model. The signal reductions are 50% for gravity residuals, while GNSS shows only half of this amount which is still very significant. Hence, during extreme conditions gravimetry can resolve the NTOL signals much better than GNSS (Figures 3a and 3b). We also replace model predictions from BSH with other NTOL data sets frequently used in

Table 1
Descriptive Statistics of the Comparison Between Observations and Non-Tidal Ocean Loading Model Values in Terms of Correlation and Reduction of Gravity Residuals (RMS) During 1 Month (26 January to 25 February 2022) With Several Storm Surges According to Figure 3

Station	Functional	BSH	AOD7	Correlation/reduction AOD7 (mGlobe)	ECCO2
Heligoland	Height-independent gravity	0.87/49%	0.77/36%	0.69/24%	0.35/6%
Onsala	Total gravity	0.80/39%	0.17/−1%	0.50/8%	0.12/8%
Serrahn	Total gravity	0.44/10%	−0.07/−9%	−0.05/−6%	0.18/0%
Strasbourg	Total gravity	0.63/19%	0.53/13%	0.40/−1%	0.19/1%
Heligoland	Vertical displacements	0.74/25%	0.69/24%	–/–	0.33/5%

the gravity community. Ocean bottom pressure anomalies from MPIOM that are also applied for the GRACE non-tidal dealiasing model AOD1B RL07 (Shihora et al., 2022) are used with SPOTL to calculate NTOL effects (denoted as AOD7). MPIOM is a baroclinic ocean model based on the primitive equations and operates on a global domain with a moderate temporal and spatial resolution (1.0° tri-polar grid and 3-hourly output) and does not employ data assimilation. Please note that these time series are currently prepared for incorporation into ATMACS (Antokoletz et al., 2024). We also utilize the publicly available Stokes coefficients of AOD1B RL07 and compute NTOL with the mGlobe package (Mikolaj et al., 2016; denoted as AOD7 (mGlobe)), and we use predictions based on ECCO2 available from the EOST loading service (Table 1).

We note that the amplitudes from AOD7 (processed with SPOTL) are much larger than the corresponding amplitudes from AOD7 (mGlobe). This is related to the mathematical approach of mGlobe. In contrast to SPOTL, which performs a convolution with load Green's functions, mGlobe calculates a truncated sum of spherical harmonic coefficients (d/o 180). This implicitly leads to an imprecise representation of the coastlines with near-coastal areas being additionally affected by the Gibbs effect. We also note an apparent time lag of 3 to 4 hr for both AOD7 solutions in comparison with the observations by shifting the AOD7 time series for maximum correlation and signal reduction indicating systematic delays in the storm surges in the German Bight in the underlying MPIOM, which is probably related to the lower resolution of MPIOM that is not sufficient to capture the high-frequency shallow-water dynamics in as much detail as high-resolution models.

The NTOL signals from all four models are computed also for the IGETS SG stations Onsala, Serrahn and Strasbourg. In total, the agreements are weaker than at Heligoland as the NTOL signals are not the primary contributor to the gravity residuals but terrestrial water storage changes coming into play in addition to instrumental disturbances in the gravity residuals automatically processed by IGETS. Again, the BSH model consistently shows by far the best agreements with the gravimetric observations and significant improvements in correlation and signal reduction on all stations from 10% (Serrahn) to 39% (Onsala). This is different for the two AOD7 solutions. Although the major NTOL peaks are visible in both solutions, AOD7 reveals deficiencies for stations near the semi-enclosed Baltic Sea (Onsala, Serrahn), while it performs well at Strasbourg which is more affected by the North Sea. However, AOD7 (mGlobe) and ECCO2 provide signal reductions of up to 8% only on any of the stations considered. We also note that the results at Strasbourg might be improved even further by combining the results from the regional BSH model with a global model like AOD7 to cover also signals from the Biskaya.

Figure 3 also reveals that vertical displacements from GNSS suffer from systematic effects and enhanced noise at subdaily time scales which greatly limits resolving the storm surge signals. The height-independent gravity residuals from iGrav 047 at Heligoland together with a mean height-to-gravity ratio for NTOL derived from the BSH model might be thus used as a proxy to estimate much more precise gravimetry-based vertical displacements that are fully independent of GNSS. The mean gravity-to-height ratio (dg/dh) at Heligoland is −2.684 (0.003) nm/s^2 per mm vertical displacement calculated from the BSH time series of height-independent gravity and vertical displacements over the investigated month with several storm surges, which is very stable and close to the results from Fratepietro et al. (2006). It should be noted that the direct Newtonian attraction of the local water mass variations has to be reduced beforehand, and this proportionality factor is still weakly dependent on the wavelength of the load (de Linage et al., 2009) and to an even lesser extent on the selected Earth model (Wang

et al., 2012). A NTOL gravity signal of 80 nm/s^2 observed with a RMSE of 2 nm/s^2 could thus be transformed into a vertical displacement of 29.8 mm with a RMSE of 0.7 mm only. This solution improves the agreement between gravimetry-based vertical displacements and BSH as well as AOD7 to end up with the same results as for gravimetry in terms of correlation and signal reduction, which appears to be a promising path for a possible incorporation of superconducting gravimeters for vertical reference frame realizations as long as local hydrological signals are small in (or sufficiently well reduced from) the gravimetric observations.

4. Conclusions

With a unique set of partially redundant geodetic instruments consisting of gravimeters, GNSS stations, and tide gauges on the small island of Heligoland in the North Sea, we demonstrate that the dedicated regional ocean model BSH-HBMnoku explains large fractions of the observed regional NTOL signals. For a particularly stormy month in winter 2022, correlations of 0.9 and signal reductions of 50% are found when reducing NTOL model predictions from gravimetric observations. This is a significant improvement against more commonly used global NTOL products provided by the EOST loading service or the mGlobe package. For stations in Central Europe, a combination of the regional model BSH-HBMnoku with a global model to include also NTOL signals from the Biskaya and the Mediterranean Sea might improve the results even further. Our analysis also provides insights into further possible improvements of global NTOL models, most notably with respect to an apparent time lag of 3 to 4 hr in AOD7 with respect to the geodetic observations. The continued operation of iGrav 047 on Heligoland will continue to provide ground truth information for future NTOL model development.

We also find that gPhoneX spring gravimeters are very well suited for the analysis of NTOL signals over periods of roughly 1 week in almost the same way as SGs, but not for longer periods due to their highly irregular drift behaviors. In view of the much lower complexity of a spring gravimeter compared to an iGrav, this opens an interesting opportunity to observe the evolution of storm surges in real-time with instruments that can be operated well sheltered away from the weather. We intend to continue this research by operating gPhoneX instruments at a number of places in close proximity to the coasts but otherwise very differing environmental conditions to further study the versatility of this instrument for oceanographic applications.

Data Availability Statement

All data sets used within this study are publicly available. Gravity and barometric pressure data from the gravimeters iGrav 047 and gPhoneX 152 at Heligoland (Voigt et al., 2020) as well as from OSG 054 at Onsala (Scherneck et al., 2022), iGrav 033 at Serrahn (Reich et al., 2024) and iOSG 023 at Strasbourg (Boy et al., 2017) are available from the IGETS database hosted by the Information System and Data Center at GFZ (Voigt et al., 2016). Raw GNSS data are available from BKG (2024), while processed data are published by Deng (2023). The sea level heights from the tide gauges HELBH and HELSH are available for the past 30 days from WSV (2024), while long time-series are available upon request from BfG (2024). The operational ocean model BSH-HBMnoku is available from BSH (2024).

References

Agnew, D. C. (2013). Spotl: Some programs for ocean-tide loading. In *Scripps institution of oceanography technical report*. University of California. Retrieved from https://igppweb.ucsd.edu/~agnew/Spotl/spotlmain.html

Antokoletz, E. D., Wziontek, H., Dobslaw, H., Balidakis, K., Klügel, T., Oreiro, A., & Tocho, C. N. (2024). Combining atmospheric and non-tidal ocean loading effects to correct high precision gravity time-series. *Geophysical Journal International*, *236*(1), 88–98. https://doi.org/10.1093/gji/ggad371

BfG. (2024). Datenstelle der Bundesanstalt für Gewässerkunde. Retrieved from Datenstelle-M1@bafg.de

BKG. (2024). The BKG GNSS data center. Retrieved from https://igs.bkg.bund.de/

Boy, J.-P. (2024). EOST loading service. Retrieved from http://loading.u-strasbg.fr

Boy, J.-P., Barriot, J.-P., Förste, C., Voigt, C., & Wziontek, H. (2020). Achievements of the first 4 years of the International Geodynamics and Earth Tide Service (IGETS) 2015–2019. In J. T. Freymueller & L. Sánchez (Eds.), *Beyond 100: The next century in geodesy. International association of geodesy symposia* (Vol. 152, pp. 107–112). Springer. https://doi.org/10.1007/1345_2020_94

Boy, J.-P., & Lyard, F. (2008). High-frequency non-tidal ocean loading effects on surface gravity measurements. *Geophysical Journal International*, *175*(1), 35–45. https://doi.org/10.1111/j.1365-246X.2008.03895.x

Boy, J.-P., Rosat, S., Hinderer, J., & Littel, F. (2017). Superconducting gravimeter data from Strasbourg—Level 1. *GFZ Data Services*. https://doi.org/10.5880/igets.st.ll.001

Brüning, T., Li, X., Schwichtenberg, F., & Lorkowski, I. (2021). An operational, assimilative model system for hydrodynamic and biogeochemical applications for German coastal waters. *Hydrographische Nachrichten/Journal of Applied Hydrography*, *118*, 6–15. https://doi.org/10.23784/HN118-01

BSH. (2024). Operational modelling of the federal Maritime and hydrographic agency (BSH). Retrieved from https://data.bsh.de/OpenData/OperationalModel/

de Linage, C., Hinderer, J., & Boy, J.-P. (2009). Variability of the gravity-to height ratio due to surface loads. *Pure and Applied Geophysics*, *166*(8–9), 1217–1245. https://doi.org/10.1007/s00024-004-0506-0

Deng, Z. (2023). Heligoland GNSS hourly time series positioning for 2017–2021. *GFZ Data Services*. https://doi.org/10.5880/GFZ.1.1.2023.001

Dill, R. (2008). Hydrological model LSDM for operational Earth rotation and gravity field variations. *GFZ ScientificTechnical Report STR08/09*. https://doi.org/10.2312/GFZ.b103-08095

Dill, R., & Dobslaw, H. (2013). Numerical simulations of global-scale high-resolution hydrological crustal deformations. *Journal of Geophysical Research: Solid Earth*, *118*(9), 5008–5017. https://doi.org/10.1002/jgrb.50353

Dobslaw, H., Bergmann-Wolf, I., Dill, R., Poropat, L., Thomas, M., Dahle, C., et al. (2017). A new high-resolution model of non-tidal atmosphere and ocean mass variability for de-aliasing of satellite gravity observations: AOD1B RL06. *Geophysical Journal International*, *211*(1), 263–269. https://doi.org/10.1093/gji/ggx302

Fenoglio-Marc, L., Scharroo, R., Annunziato, A., Mendoza, L., Becker, M., & Lillibridge, J. (2015). Cyclone Xaver seen by geodetic observations. *Geophysical Research Letters*, *42*(22), 9925–9932. https://doi.org/10.1002/2015GL065989

Fratepietro, F., Baker, T. F., Williams, S. D. P., & Van Camp, M. (2006). Ocean loading deformations caused by storm surges on the Northwest European shelf. *Geophysical Research Letters*, *33*(6), L06317. https://doi.org/10.1029/2005GL025475

Klügel, T., & Wziontek, H. (2009). Correcting gravimeters and tiltmeters for atmospheric mass attraction using operational weather models. *Journal of Geodynamics*, *48*(3–5), 204–210. https://doi.org/10.1016/j.jog.2009.09.010

Mikolaj, M., Meurers, B., & Güntner, A. (2016). Modelling of global mass effects in hydrology, atmosphere and oceans on surface gravity. *Computers & Geosciences*, *93*, 12–20. https://doi.org/10.1016/j.cageo.2016.04.014

Olsson, P.-A., Scherneck, H.-G., & Ågren, J. (2009). Effects on gravity from non-tidal sea level variations in the Baltic Sea. *Journal of Geodynamics*, *48*(3–5), 151–156. https://doi.org/10.1016/j.jog.2009.09.002

Reich, M., Güntner, A., & Schröder, S. (2024). Superconducting gravimeter data from Serrahn—level 1. *GFZ Data Services*. https://doi.org/10.5880/igets.se.l1.001

Scherneck, H.-G., Mouyen, M., & Reldin, J. (2022). Superconducting gravimeter data from Onsala—Level 1. *GFZ Data Services*. https://doi.org/10.5880/igets.os.l1.001

Schueller, K. (2015). Theoretical basis for Earth tide analysis with the new ETERNA34-ANA-V4.0 program. *Bulletin d'Information des Marées Terr*, *149*, 12024–12061. http://maregraph-renater.upf.pf/bim/BIM/bim149.pdf

Schueller, K. (2020). Program System ETERNA-x et34-x-v80 for Earth and ocean tides analysis and prediction. In *Documentation manual 01: Theory and 02: Users guide*. Technical Reports, Institution. Retrieved from http://ggp.bkg.bund.de/eterna?download=7283

Schulzweida, U. (2022). CDO user guide. *Zenodo*, *2*(1.0). https://doi.org/10.5281/zenodo.7112925

Shihora, L., Balidakis, K., Dill, R., & Dobslaw, H. (2022). Atmosphere and Ocean non-tidal Dealiasing level-1B (AOD1B) product RL07. *GFZ Data Services*. https://doi.org/10.5880/GFZ.1.3.2022.003

Voigt, C., Förste, C., Wziontek, H., Crossley, D., Meurers, B., Palinkas, V., et al. (2016). *Report on the data base of the International Geodynamics and Earth Tide Service (IGETS), Scientific Technical Report STR Potsdam*. GFZ German Research Centre for Geosciences. https://doi.org/10.2312/gfz.b103-16087

Voigt, C., Stolarczuk, N., Pflug, H., Förste, C., Flechtner, F., Peters, H., & Fietz, M. (2020). Superconducting gravimeter data from Helgoland—level 1. *GFZ Data Services*. https://doi.org/10.5880/igets.he.l1.001

Voigt, C., Sulzbach, R., Timmen, L., Dobslaw, H., Weise, A., Deng, Z., et al. (2023). A superconducting gravimeter on the island of Heligoland for the high-accuracy determination of regional ocean tide loading signals of the North Sea. *Geophysical Journal International*, *234*(3), 1585–1602. https://doi.org/10.1093/gji/ggad147

Wang, H., Xiang, L., Jia, L., Jiang, L., Wang, Z., Hu, B., & Gao, P. (2012). Load Love numbers and Green's functions for elastic Earth models PREM, iasp91, ak135, and modified models with refined crustal structure from Crust 2.0. *Computers and Geosciences*, *49*, 190–199. https://doi.org/10.1016/j.cageo.2012.06.022

Weise, A., Timmen, L., Deng, Z., Gabriel, G., Rothleitner, C., Schilling, M., & Voigt, C. (2020). Observing Ocean mass variability with spring gravimeters – Storm surge induced signals on the North Sea island Helgoland. *AVN: Allgemeine Vermessungs-Nachrichten*, *127*(4), 163–173.

Wessel, P., & Smith, F. (1998). New, improved version of generic mapping tools released. *Eos*, *79*(47), 579. https://doi.org/10.1029/98EO00426

WSV. (2024). Pegelonline. Retrieved from https://www.pegelonline.wsv.de/webservices/files/Wasserstand+Rohdaten/NORDSEE